Supplementary Information

Fluorescence-lifetime encoding for scalable single-protein-resolution imaging

Alessia Gentili [1†], Robert Hollmann[1†], Cecilia Zaza[1], Harry Holmes[1,2], Karol Kołątaj[3,4], David J. Williamson[2], Irene Carlon-Andres[2,5], Tomas Malinauskas[6], Guillermo P. Acuna[3,4], Sergi Padilla-Parra[2,7,8], and Sabrina Simoncelli[1,9]*

1. London Centre for Nanotechnology, University College London, London WC1H 0AH, United Kingdom.
2. Department of Infectious Diseases, School of Immunology & Microbial Sciences, King's College London, London SE1 9RT, United Kingdom.
3. Swiss National Center for Competence in Research (NCCR) Bio-inspired Materials, University of Fribourg, Fribourg, Switzerland.
4. Department of Physics, University of Fribourg, Fribourg, Switzerland.
5. The Rosalind Franklin Institute, Harwell Campus, Didcot OX11 0QS, United Kingdom
6. MRC Laboratory of Molecular Biology, Francis Crick Avenue, Cambridge CB2 0QH, United Kingdom
7. Instituto Biofisika (EHU, CSIC), University of the Basque Country, Leoia, E-48940, Spain.
8. Ikerbasque, Basque Foundation for Science, Bilbao 48013, Spain.
9. Department of Chemistry, University College London, London, WC1H 0AJ, United Kingdom.

† Equal Contribution

Supplementary Figures

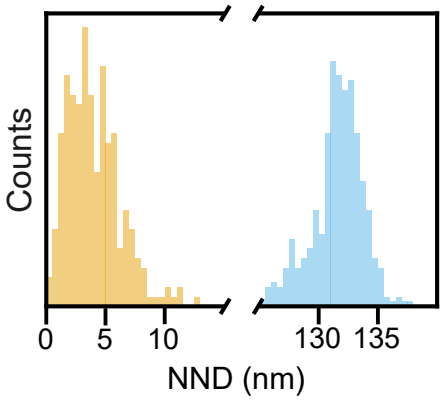

Supplementary Figure 1. RESI nearest-neighbour distance analysis recovers the designed 3.2 nm intra-pair separation, consistent with RE-FLIM. First- and second-nearest-neighbour distance (NND) analysis of RESI-resolved docking-strand pairs on DNA origami (*n* = 267 docking pairs), imaged sequentially by TIRF microscopy using an sCMOS camera (Extended Data 2). The distribution recovers the designed intra-pair separation (1st NND = 3.3 nm) and inter-pair spacing (2nd NND = 131.3 nm), in agreement with RE-FLIM measurements obtained on the same structure in a single acquisition round (Fig. 1f).

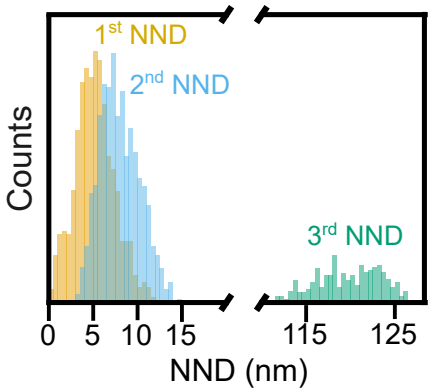

Supplementary Figure 2. RESI nearest-neighbour distance analysis recovers the designed ~5.5 nm intra-trimer separation, consistent with RE-FLIM. First-, second-, and third-nearest-neighbour distance (NND) analysis of RESI-resolved docking-strand trimers on DNA origami (*n* = 205 docking triangles), imaged sequentially by TIRF microscopy using an sCMOS camera (Extended Data 4). The distribution recovers the designed intra-trimer separation (1st NND = 5.3 nm; 2nd NND = 7.3) and inter-pair spacing (3rd NND = 118.3 nm), in agreement with RE-FLIM measurements obtained on the same structure in a single acquisition round (Fig. 1i).

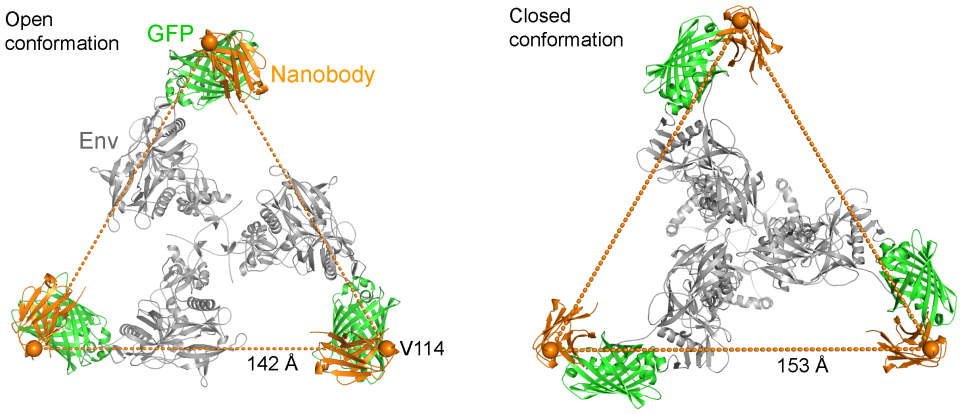

Supplementary Figure 3. Superposition of AlphaFold models of Env-GFP–nanobody complexes onto the open and closed conformations of the HIV-1 Env trimer. AlphaFold 3 models of the HXB2 Env-V4-GFPopt–nanobody binary complex were superposed onto HIV-1 Env trimers representing the closed (PDB ID: 5T3X) and open (PDB ID: 5VN3) conformations using the conserved Env α-helix (Met100–Leu116). Distances between the Cα atoms (shown as spheres) of Val114 in the anti-GFP nanobody are indicated by dashed lines. Asparagine-linked glycans, the N- and C-terminal regions of Env construct, and the nanobody His6-tag are omitted for clarity.

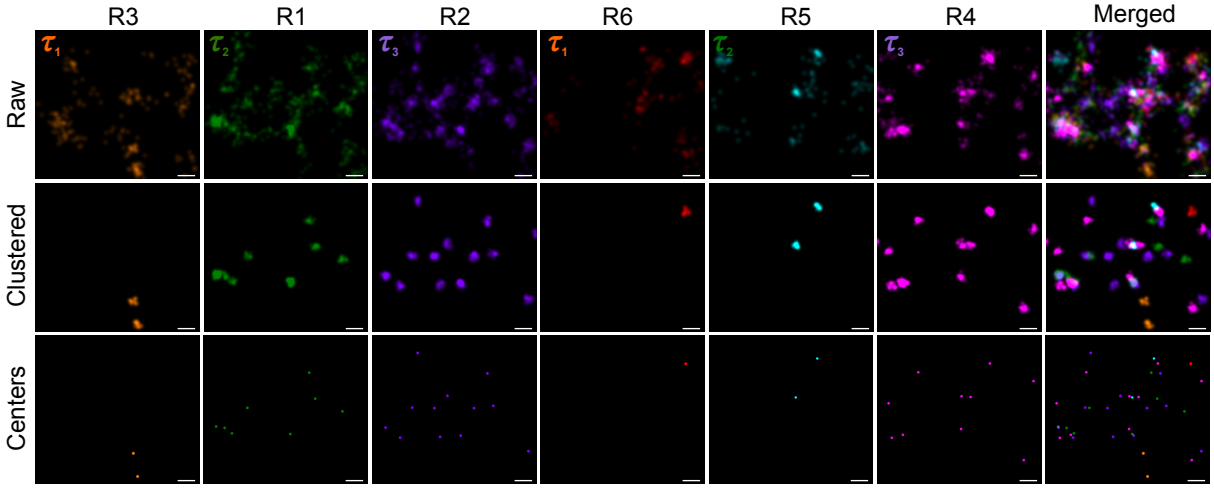

Supplementary Figure 4. Step-by-step single-channel analysis of barcode separation. Zoomed-in region of HXB2 Env-V4-GFP$_{OPT}$ expressed in U2OS cells and stochastically labelled with anti-GFP nanobodies bearing six orthogonal docking strands (R1–R6), resolved by two rounds of exchange combined with simultaneous lifetime multiplexing (τ_1– τ_3 per round) into six individual barcode channels. For each channel, raw localizations ("Raw"), SMLM clustered localizations ("Clustered") and cluster centres ("Centres") are shown; the rightmost column shows all six channels merged, retaining their assigned barcode colour. Scale bars, 100 nm

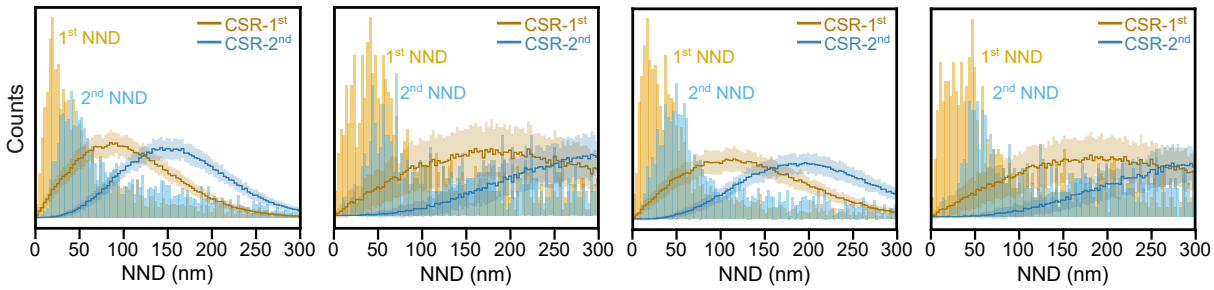

Supplementary Figure 5. Nearest-neighbor distance analysis of RE-FLIM-resolved Env centers across independent fields of view. First- and second-order nearest-neighbor distance (NND) distributions of detected RE-FLIM Env centers from four independent fields of view, compared with complete spatial randomness (CSR) simulations (mean ± s.d. of 100 simulated datasets, each comprising all four fields of view). The distributions reveal short-range clustering of labelled Env protomers relative to spatially random distributions.

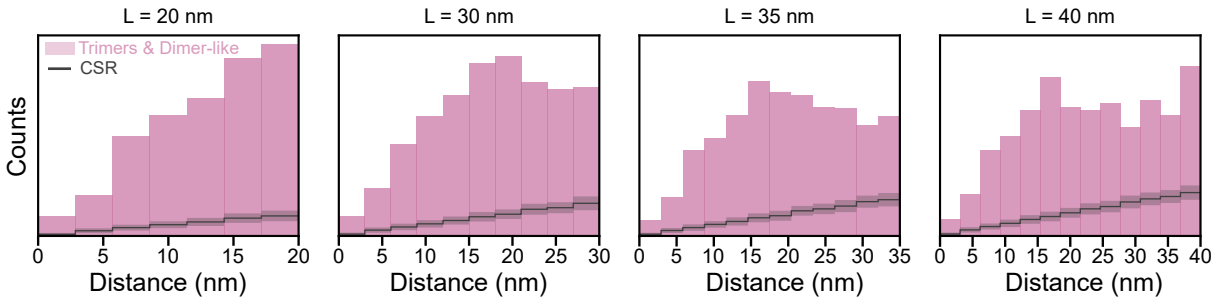

Supplementary Figure 6. Env centroid separations show an intrinsic, linking-radius-invariant length scale absent in density-matched random simulations. All pairwise separations within graph-classified dimer-like and trimer groups of RE-FLIM-resolved Env centroids (*n* = 8055 centroids from four independent fields of view), at linking distances (L) of 20, 30, 35 and 40 nm. Grey, the same analysis applied to density-matched complete spatial randomness (CSR) simulations (mean ± s.d. of 100 simulated datasets, each comprising all four fields of view). Env yields substantially more classified groups than CSR at every linking distance (Supplementary Table 3). Across L = 20–40 nm, the modal Env protomer separation remained confined to 16.0–19.5 nm (18.6, 17.2, 19.5, 16.0 and 16.9 nm at L = 20, 25, 30, 35 and 40 nm, respectively), while the modal CSR separation tracked the linking radius itself (18.6, 23.4, 28.5, 33.5 and 38.5 nm at the same radii), as expected for a distribution with no intrinsic length scale. At L = 20 nm the two modes coincide because the window edge truncates the Env distribution before its natural peak; at wider radii the Env mode remains stable even as the growing CSR mode and coincidence background increasingly overlap it, indicating a genuine, radius-independent length scale in the Env data.

Supplementary Tables

Supplementary Table 1. List of modified staple strands used for the DNA origami containing two pairs of DNA-PAINT docking sites separated by 3.2 nm. For DNA-PAINT docking strand staples (red), the 5′ spacer sequence is shown before the docking strand sequence complementary to the corresponding DNA-PAINT imager strand. Biotin-modified staples were used for the DNA-origami surface immobilization.

Staple Name	Sequence
Right R1	TCGTAATCATCCGCTCATGAATCGGCCAACGCGCGGGGAGAGTTTTCCTCCTCCTCCTC CTCCT
Right R4	AAGAACTCCAATATTAGTCACACGACCAGTA CA ACACACACACACACACACA
Left R1	CGGCTTAGGCAAATCCATGGTTTGAAATACCGACCGTGTGCCATTTCCTCCTCCTCCTCC TCCT
Left R4	TGAGCGCTTAAGCCCATGGCATGATTAAGACT CA ACACACACACACACACACA
Biotin 1	CACTAAAACACTCACGAACTAACACTAAAGT - Biotin-TEG
Biotin 2	TCACGACGTTGGGCGCTTTGGTAAAAC - Biotin-TEG
Biotin 3	ACAGGAAGATTGTCCCCCTTATTCACCCTCATTTGTTTC - Biotin-TEG
Biotin 4	GTTGATAGATATAAGCATAAGTATAGC - Biotin-TEG
Biotin 5	CAGAGATAGCGATAGTGAATAACATAA - Biotin-TEG
Biotin 6	AGAGTACTCACGCTAACCTTTAATTGC - Biotin-TEG

Supplementary Table 2. List of modified staple strands used for the DNA origami containing three DNA-PAINT docking sites arranged in ~5.5 nm triangles. For DNA-PAINT docking strand staples (red), the 5′ spacer sequence is shown before the docking strand sequence complementary to the corresponding DNA-PAINT imager strand. Biotin-modified staples were used for the DNA-origami surface immobilization.

Staple Name	Sequence
Left R1	AATATTGACGTCACCGTGCGTAGATTTTCAGGTTTCCTCCTCCTCCTCCTCCT
Left R2	ATTATCACCGGAAATGTTAGCAAACGTAGAAAAACCACCACCACCACCACCA
Left R3	TGAGCGCTTAAGCCCATGGCATGATTAAGACTTCCTCTCTCTCTCTCTCTCTC
Centre Left R2	CAGAACCGCATGTACCGCTAAACAACTTTCAATTACCACCA
Centre Right R2	AGCTCAACGAACGAGTGGCAAGGCAAAGAATTTTACCACCA
Right R1	ACGTTGGTGGATTGACGGTCAGTTGGCAAATCTTTCCTCCTCCTCCTCCTCCT
Right R2	CAAACGGCGTAGATGGCGCAACTGTTGGGAAGAAACCACCACCACCACCACCA
Right R3	AAATTGTTATGGTCATCTCTTCGCTATTACGCTCCTCTCTCTCTCTCTCTCTC
Biotin 1	CACTAAAACACTCACGAACTAACACTAAAGT - **Biotin-TEG**
Biotin 2	TCACGACGTTGGGCGCTTTGGTAAAAC - **Biotin-TEG**
Biotin 3	ACAGGAAGATTGTCCCCCTTATTCACCCTCATTTGTTTC - **Biotin-TEG**
Biotin 4	GTTGATAGATATAAGCATAAGTATAGC - **Biotin-TEG**
Biotin 5	CAGAGATAGCGATAGTGAATAACATAA - **Biotin-TEG**
Biotin 6	AGAGTACTCACGCTAACCTTTAATTGC - **Biotin-TEG**

Supplementary Table 3. Number of dimer-like groups and closed triangles as a function of the linking radius (L). Counts are pooled across four fields of view (*n* = 8055 RE-FLIM-resolved Env centroids), classified as described in Methods. CSR values are the mean ± s.d. of 100 density-matched complete spatial randomness simulations, each comprising all four fields of view.

L (nm)	***Dimer-like***		***Trimer***	
	Env	*CSR*	*Env*	*CSR*
20	585	68 ± 8	37	0.3 ± 0.6
25	711	105 ± 10	62	1 ± 1
30	761	148 ± 13	106	2 ± 1
35	767	198 ± 14	123	3 ± 2
40	790	251 ± 16	164	5 ± 2

Supplementary Notes

Supplementary Note 1: Event-based analysis of RE-FLIM data

Overview and input data structure

RE-FLIM event analysis was performed using a custom Python-based pipeline designed to extract spatial and fluorescence lifetime information from individual DNA-PAINT binding events directly from the continuous photon stream recorded by the LINCam detector.

The analysis uses three input files generated during preprocessing: (i) a localization file containing preliminary single-molecule localizations obtained using Picasso Localize, (ii) a photon index file containing the time-ordered stream of individual photon events, including detector coordinates and TCSPC arrival-time channels, and (iii) a drift correction file generated during localization analysis.

Localizations were assigned to groups corresponding to individual structures or regions of interest (ROIs). These groups were defined either manually from reconstructed localization images or using automated clustering procedures. Event analysis was subsequently performed separately for each group.

Linking localizations into binding events

Within each group, preliminary localizations were linked into candidate DNA-PAINT binding events based on temporal continuity and spatial proximity. Localizations occurring within adjacent or nearby frames were assigned to the same event when they satisfied both temporal and spatial criteria.

The maximum allowed temporal separation between linked localizations was one dark frame. Spatial linking was performed using an uncertainty-scaled proximity criterion based on the localization precision values obtained from Picasso (lpx and lpy), such that localizations with greater positional uncertainty were permitted a proportionally larger linking distance. Specifically, two localizations were linked if their separation was less than or equal to twice the sum of their localization precisions ($2 \times (lpx + lpy)$). Localizations that could not be linked to any other localization were excluded from further analysis.

Each linked event was condensed into a single summary entry containing parameters derived from the contributing Picasso localizations. The preliminary event position was calculated as the photon-weighted average of the localization coordinates. The frame number, photon count, net gradient, ellipticity and preliminary localization precision were assigned from the brightest localization within the event (defined as the localization with the highest photon count), whereas the background value was calculated as the mean background across all localizations contributing to the event.

The first and last localization frames of each event were converted into approximate start and end times using the oversampled frame timing. These preliminary parameters were used only to initialize subsequent photon-level analysis. The preliminary position defined the spatial region from which event photons were retrieved and was subsequently replaced by a photon centre-of-mass localization. The corresponding localization uncertainty was recalculated as the standard error of the mean photon coordinates. Similarly, the approximate event boundaries were refined by change-point analysis of the photon intensity-time trace.
The photon-weighted PSF width obtained from the preliminary localization analysis was retained for the Gaussian weighting procedure used during lifetime estimation.

Photon retrieval and drift correction
Event-level spatial and temporal information was refined using the original photon stream. Because RE-FLIM datasets can contain tens of gigabytes of photon data, the indexed photon stream was loaded once, and drift correction and event assignment were then performed sequentially for each group on the subset of photons within its ROI, rather than processing the full photon stream at once.

For each group, photons within the corresponding ROI were extracted from the indexed photon stream and corrected for sample drift using the experimentally determined drift trace. The drift-corrected photon coordinates were transformed into the same coordinate system as the corrected Picasso localizations.

Following photon retrieval, photons belonging to individual events were identified by spatial cropping around the preliminary event position and temporal selection based on the approximate frame-derived event boundaries; these boundaries were subsequently refined by change-point analysis (next section), and the refined limits defined the photons used for position and lifetime estimation.

Determination of event temporal boundaries
The temporal limits of each binding event were refined directly from the photon intensity time trace. Photon arrival times were binned into 10 ms intervals and smoothed using a one-dimensional Lee filter.

Change-point detection was performed using binary segmentation with an L2 cost function, with two change points used to identify the transition between background and fluorescence states. The resulting transition points defined the fluorescence onset, termination, and event duration. If change-point detection failed, the full photon arrival-time range associated with the candidate event was used as a fallback.

Photon-based event localization
Following temporal refinement, event positions were recalculated directly from the assigned photons. Photons detected before the calibrated excitation pulse peak were

excluded. The remaining photons were restricted to a circular ROI centred on the preliminary event position. The event position was calculated as the photon centre of mass of the assigned photon coordinates. The localization uncertainty (σ_{SMLM}) was calculated as the standard error of the mean photon coordinates in the *x* and *y* directions.

Fluorescence lifetime estimation

Fluorescence lifetime was estimated from the photon arrival-time distribution of each binding event using a spatially weighted approach. Photon microtimes (TCSPC channels) within the event ROI were weighted according to their radial distance from the fitted event position using a Gaussian mask, with photons closer to the event centre contributing more to the lifetime estimate. The Gaussian weighting width (σ) was defined from the PSF width obtained during the preliminary localization analysis.

The event lifetime was calculated as the weighted mean photon arrival-time relative to the excitation pulse peak. An effective photon number was calculated from the weighting distribution, and the lifetime uncertainty was estimated as the weighted standard deviation of photon arrival times divided by the square root of this effective photon number.

Lifetime values were reported in TCSPC channels, with each channel corresponding to 10 ps. The excitation pulse peak position was determined once per dataset from the mode of the photon arrival-time histogram generated from the first 1 million detected photons.

Brightness and local brightness normalization (optional)

Event photon counts were background-corrected by subtracting the expected background contribution, calculated as the mean Picasso background estimate of the event's localizations scaled by the event duration and the area of the position-fitting ROI. Event brightness was calculated as the background-corrected photon count per millisecond of event duration. When enabled, a smooth spatial brightness map was generated from all detected events using inverse-distance weighting over a fixed neighbourhood radius on a grid spanning the field of view. Each event brightness value was normalized by the corresponding local brightness estimate to correct for spatial variations in excitation intensity, including the Gaussian illumination profile across the field of view. For events with an associated lifetime measurement, the lifetime-to-normalized-brightness ratio was additionally recorded.